B meson Decay Constants Using Relativistic Heavy Quarks

Matthew Black[*] **and Oliver Witzel**

(RBC and UKQCD collaborations)

Center for Particle Physics Siegen, Theoretische Physik 1, Naturwissenschaftlich-Technische Fakultät, Universität Siegen, 57068 Siegen, Germany

E-mail: matthew.black@uni-siegen.de

We present an update on ongoing work to extract pseudoscalar and vector decay constants for $B^{(*)}$, $B_s^{(*)}$ and $B_c^{(*)}$ mesons and determine phenomenologically-interesting ratios such as f_{B_s}/f_B or f_{B^*}/f_B. Our calculation is based on $N_f = 2 + 1$ dynamical flavour gauge field ensembles generated by the RBC/UKQCD collaborations using domain-wall fermions and the Iwasaki gauge action. Using domain-wall light, strange, and charm quarks and relativistic b quarks, we obtain results at multiple lattice spacings and valence quark masses.

The 39th International Symposium on Lattice Field Theory,
8th-13th August, 2022,
Rheinische Friedrich-Wilhelms-Universität Bonn, Bonn, Germany

---

[*]Speaker

1. Introduction

Leptonic decays of B mesons are some of the simplest flavour-changing processes in which a b quark can participate. In the Standard Model (SM), the decay rate of a B^+ meson decaying into a charged-lepton–neutrino pair is given by

$$\Gamma(B^+ \to \ell^+ \nu_\ell) = \frac{G_F^2 m_B m_\ell^2}{8\pi} \left(1 - \frac{m_\ell^2}{m_B^2}\right)^2 |V_{ub}|^2 f_B^2. \tag{1}$$

From the perspective of QCD, this is a very clean process where all of the nonperturbative, hadronic physics is contained within the decay constant f_B. The simplicity of Eq.(1) would motivate using these decay rates to determine the CKM matrix element $|V_{ub}|$, however this requires high precision knowledge of both the measured decay rate and the decay constant f_B. The limiting factor in this respect is still experiment where thus far $B^+ \to \tau^+ \nu_\tau$ and $B^+ \to \mu^+ \nu_\mu$ have been observed with precision $\sim 30\%$ and 40% respectively [1–6]; this precision is anticipated to be improved upon in the near-future using the new data being collected by Belle II. The pseudoscalar decay constants of B mesons with a light/strange valence quark are well-studied using nonperturbative methods. From QCD sum rules, the best determinations have a precision $\sim 10\%$ [7–9]. With lattice QCD, these are currently known to a precision of less than 1% [10–14]; from the pseudoscalar decay constants also comes the important SU(3)-breaking ratio f_{B_s}/f_B. Furthermore, these decay constants are important in other processes such as in extracting bag parameters of neutral B-meson mixing from hadronic matrix elements or in predicting the rare leptonic decays $B_q \to \ell^+ \ell^-$.

As well studied as the pseudoscalar decay constants are, one can also consider the decay constants of more 'exotic' B states. As the next generation of experiments begin, such as HL-LHC and Belle II, and further theoretical techniques allow the community to predict more 'exotic' decay channels, there is more motivation than ever to develop high-precision lattice calculations of new decay constants, with lower-hanging 'exotic' fruits being for example the heavier B_c meson and the vector states B_q^*, $q = l, s, c$. To date, only one calculation of the pseudoscalar B_c decay constant has been performed by the HPQCD collaboration [15]. Similarly, there exists only two lattice calculations of the decay constant for the vector meson state B_q^* from the HPQCD [15] and ETM [16] collaborations. Of additional interest in the case of the vector decay constant is that these two calculations (with $q = l, s$) are in tension with one another and in fact their ratios $f_{B_{(s)}^*}/f_{B_{(s)}}$ lie to opposite sides of unity. The single calculation of f_{B_c} and the tension in $f_{B_{(s)}^*}$ motivates further lattice calculations of these quantities to first reach consensus on their values and then push to higher precision. We will contribute to this by analysing the pseudoscalar and vector decay constants for B, B_s, and B_c mesons.

2. Lattice calculation

We use seven RBC/UKQCD 2+1-flavour domain-wall fermion (DWF) and Iwasaki gauge field ensembles with four lattice spacings $a \sim 0.11, 0.08, 0.07, 0.06\,\mathrm{fm}$ (determined from RBC/UKQCD analyses [17–19]) and pion masses $\in [267, 433)\,\mathrm{MeV}$. Light and strange quarks are simulated with the Shamir DWF action with $M_5 = 1.8$. These ensembles are listed in Table 1.

	L	T	L_s	a^{-1}/GeV	am_l^{sea}	am_s^{sea}	M_π/MeV	# cfgs	# sources
C1	24	64	16	1.785	0.005	0.040	340	1636	1
C2	24	64	16	1.785	0.010	0.040	433	1419	1
M1	32	64	16	2.383	0.004	0.030	302	628	2
M2	32	64	16	2.383	0.006	0.030	362	889	2
M3	32	64	16	2.383	0.008	0.030	411	544	2
F1S	48	96	12	2.785	0.002144	0.02144	267	98	24
X1	32	64	12	3.148	0.0047	0.0186	371	40	16

Table 1: Ensembles used for the simulations reported here [17, 18, 20, 21]. am_l^{sea} and am_s^{sea} are the light and strange sea quark masses and M_π is the unitary pion mass. Valence strange quarks are near their physical mass.

As bottom quarks are too heavy to be simulated directly at their physical value on these lattices, we choose the effective action approach in order to simulate physical b quarks. Specifically, we choose the relativistic heavy quark (RHQ) action, which is the Columbia variant [22, 23] of the Fermilab heavy-quark action [24], with three nonperturbatively-tuned parameters m_0a, c_P, and ζ [25]. The tuning of these parameters on each ensemble was initially carried out in Ref. [25]; we report here first results for tuning the RHQ parameters on the X1 ensemble. Charm quarks are simulated with the Möbius DWF action and $M_5 = 1.6$ [18, 19, 26, 27]. We use three masses below m_c^{phys} on C and two masses bracketing m_c^{phys} on M, F, and X. Light and strange quarks have point sources, while the b and c quarks use Gaussian-smeared sources and point or smeared sinks; to improve statistics on X, instead of point sources we use Z2-noise wall sources which are also Gaussian-smeared for the b quarks.

Here we consider the vacuum-to-meson matrix elements of B_q mesons at rest (where $q = l, s, c$ denotes the valence quark) $\langle 0|J_\mu|B_q(0)\rangle$ for the axial-vector A_μ and vector V_μ currents to yield the decay constants of the pseudoscalar and vector meson states respectively, where for the pseudoscalar we require only the temporal component A_0 and for the vector the spatial components V_i, $i = 1, 2, 3$. For these matrix elements, we can relate a lattice current J_μ to the renormalised current $\mathcal{J}_\mu$ via the multiplicative renormalisation factor

$$Z_{J_\mu}^{bq} = \rho_{J_\mu}^{bq} \sqrt{Z_V^{qq} Z_V^{bb}}, \tag{2}$$

which follows the partially-nonperturbative approach [28, 29] where Z_V^{bb} and Z_V^{qq} are nonperturbatively calculated and $\rho_{J_\mu}^{bq}$ is the remaining correction calculated perturbatively at one-loop and is expected to only deviate from unity by $O(1\%)$ [30, 31]. For DWFs, Z_V^{qq} can be computed via the relation

$$Z_V^{qq} = Z_A^{qq} + O(am_{\text{res}}), \tag{3}$$

and Z_V^{bb} is calculated from the matrix element

$$Z_V^{bb}\langle B_q|V_0|B_q\rangle = 2M_{B_q}. \tag{4}$$

3
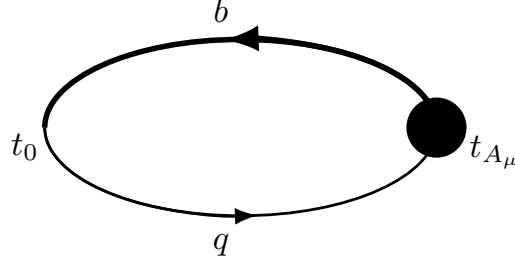
Figure 1: Two-point correlator used to determine a pseudoscalar decay amplitude. t_0 indicates the position of the source with pseudoscalar current $\bar{b}\gamma_5 q$, and t_{A_μ} is the time of insertion of the axial-vector current A_μ.

Using the RHQ action, in order to reduce cut-off effects we require for lattice (axial-)vector currents to include $O(a)$-improvement terms before this renormalisation. For the spatial components of the vector current $V_i = \bar{b}\gamma_i q$, the relevant subset of the $O(a)$-improvement operators for calculating the decay constant are

$$V_i^0 = \bar{b}\gamma_i q, \qquad V_i^2 = \bar{b}(2\overleftarrow{D}_i)q, \qquad V_i^4 = \bar{b}\gamma_i \sum_j \gamma_j (2\overleftarrow{D}_j)\, q, \qquad (5)$$

and similarly for the axial-vector current $A_0 = \bar{b}\gamma_0\gamma_5 q$ replacing $\gamma_i \to \gamma_0\gamma_5$. By considering only the temporal component, A_0^2 is eliminated using the equations of motion. Then, we can write the required $O(a)$-improved currents as

$$A_0 = A_0^0 + c_A^4 A_0^4, \qquad (6)$$

$$V_i = V_i^0 + c_V^2 V_i^2 + c_V^4 V_i^4. \qquad (7)$$

The coefficients $c_{A,V}^k$ of the $O(a)$-improvement operators are computed at one-loop perturbation theory [30, 31].

The renormalised vacuum-to-meson matrix elements are related to the decay constants as

$$\langle 0|\mathcal{A}_0|B_q(0)\rangle = f_{B_q} M_{B_q}, \qquad (8)$$

$$\langle 0|\mathcal{V}_i|B_{q,j}^*(0)\rangle = f_{B_q^*} M_{B_q^*} \delta_{ij}. \qquad (9)$$

It can be simpler first to consider the decay amplitude $\Phi_{B_q} = f_{B_q}\sqrt{M_{B_q}}$ which can be defined as a ratio of two-point correlators in the limit of $t_0 \ll t \ll T + t_0$ such that excited states have decayed and the ground state of the system is clearly resolved. By 'folding' correlators such that they only have forwards-propagating states up to extent $T/2$ and $t_0 = 0$, we need only consider the limit $t \gg 0$ to find the ground state. For pseudoscalar and vector decay amplitudes respectively, these ratios are defined as

$$\Phi_{B_q} = \sqrt{2}\, Z_{A_0}^{bq} \lim_{t \gg 0} \frac{|\tilde{C}_{A_0 P}(t, 0)|}{\sqrt{\tilde{C}_{PP}(t, 0)\, e^{-M_{B_q} t}}}, \qquad (10)$$

$$\Phi_{B_q^*} = \sqrt{2}\, Z_{V_i}^{bq} \lim_{t \gg 0} \frac{|\tilde{C}_{V_i V_i}(t, 0)|}{\sqrt{\tilde{C}_{V_i^0 V_i^0}(t, 0)\, e^{-M_{B_q^*} t}}}, \qquad (11)$$

where we define P the pseudoscalar current $\bar{b}\gamma_5 q$ and a two-point correlation function $C_{XY}(t, t_0)$ with currents X, Y inserted at times t, t_0 respectively. $\tilde{C}$ indicates the correlator is smeared at the source, and $\tilde{\tilde{C}}$ indicates both source and sink are smeared. A schematic of the two-point correlator $C_{A_0 P}(t, t_0)$ is shown in Figure 1.

Finally, we present the decay amplitudes as dimensionless ratios over the B_s meson mass $M_{B_s}^{3/2}$, which is used to tune the RHQ parameters to the physical value of the b quark. To gain our final results in physical units after performing continuum extrapolations, we can simply multiply by the experimental value of M_{B_s} [32]. In Figure 2, we show examples of the effective mass $M_{B_s^{(*)}}$ and dimensionless bare decay amplitude $\Phi_{B_q^{(*)}}/M_{B_s}^{3/2}$.
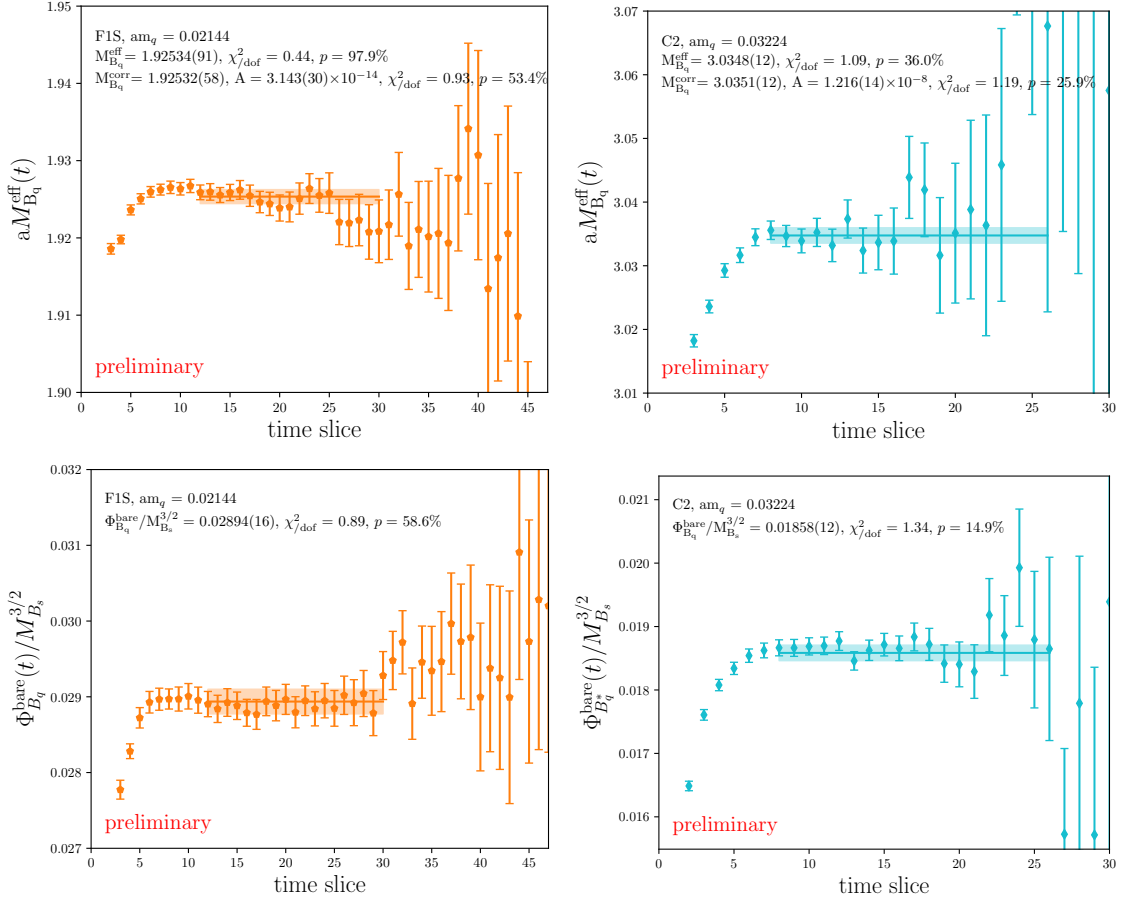
Figure 2: Determination of the effective mass (top) and dimensionless decay amplitude (bottom) for the pseudoscalar on F1S (left) and for the vector on C2 (right). The data are fitted to a constant value in the region where excited state contamination is minimised and we have a clear ground state signal.

3. Chiral and Continuum Extrapolations

Here we show the current status of our analysis to extrapolate to the physical values for the decay amplitudes of pseudoscalar $B_{(s)}$ systems. Analysis of the B_c follows analogously with an extra-/interpolation to physical charm mass using the η_c meson mass. Measurements are still

in progress for the vector states and thus extra-/interpolations to physical values cannot yet be performed.

For the determination of Φ_{B_s} we currently consider a two step procedure. First we correct for slight mistunings of the used strange quark mass by inter-/extrapolating to the physical value. That way we obtain values for Φ_{B_s} for each of our six different ensembles and use these values to also form SU(3) symmetry breaking ratios Φ_{B_s}/ϕ_B. In order to determine f_{B_s} we need to renormalize our Φ_{B_s} values and then perform in a second step a continuum limit extrapolation in a^2.

Skipping the renormalisation of the decay amplitudes for now, we continue looking at the SU(3) symmetry breaking ratio Φ_{B_s}/Φ_B right away. To perform an extrapolation of our data shown in Figure 3, we use NLO SU(2) Heavy Meson Chiral Perturbation Theory (HMχPT). For sufficiently light valence quark masses, this will provide an effective description of the decay amplitude as a function of the pion mass. This allows us to take the joint continuum and physical pion mass limit from our data. Similarly we use HMχPT to also calculate the SU(3)-breaking ratio f_{B_s}/f_B In the limit of unitary pions, our fit Ansätze for these extrapolations are

$$\frac{\Phi_{B_x}}{M_{B_s}^{3/2}} = \Phi_0 \left\{ 1 - \frac{1+3g_b^2}{(4\pi f_\pi)^2} \frac{3}{4} \cdot M_{xx}^2 \ln(M_{xx}^2/\Lambda_\chi^2) + c_1 \cdot \frac{2M_{xx}^2}{(4\pi f_\pi)^2} + c_2 \cdot \frac{a^2}{(4\pi f_\pi)^2} \right\}, \quad (12)$$

$$\frac{\Phi_{B_s}}{\Phi_{B_x}} = R_\Phi \left\{ 1 + \frac{1+3g_b^2}{(4\pi f_\pi)^2} \frac{3}{4} \cdot M_{xx}^2 \ln(M_{xx}^2/\Lambda_\chi^2) \right\} + d_1 \cdot \frac{2M_{xx}^2}{(4\pi f_\pi)^2} + d_2 \cdot \frac{a^2}{(4\pi f_\pi)^2}, \quad (13)$$

where $\Phi_0, c_1, c_2, R_\Phi, d_1, d_2$ are fit coefficients, M_{xx} is the mass of a pion with two valence quarks of mass m_x, $g_b = 0.56(3)$ the $B^*B\pi$ coupling constant [33], and $f_\pi = 130.2(1.2)$ MeV the pion decay constant [34]. The chiral-continuum extrapolation for Φ_{B_s}/Φ_{B_x} is shown in Figure 3
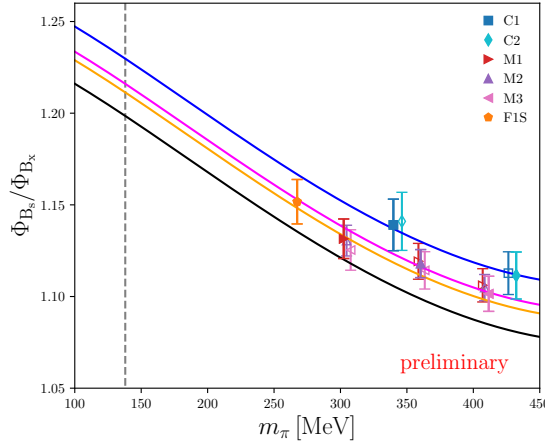
Figure 3: Chiral-continuum extrapolation of Φ_{B_s}/Φ_{B_q} using NLO SU(2) HMχPT. The coloured data are associated with different gauge configurations as indicated in the legend. Only the filled points (unitary) enter the fits. The coloured lines indicate the fit function at each corresponding lattice spacing, the black line indicates the function at zero lattice spacing. The black dashed line indicates the isospin-averaged pion mass, $m_{\bar\pi} \sim 138$ MeV. Only statistical errors are shown.

It is also possible for the above fits to choose different Ansätze to perform our extrapolations. The variation of results from different Ansätze will be included in a full systematic error analysis

later on. Further systematic effects to be considered include, for example, sea quark mass mistuning and RHQ parameter uncertainties.

4. Tuning RHQ on X1

In early analysis of the B_c decay constant using C, M, and F ensembles, large cut-off effects are found, particularly on the coarse C ensembles. Therefore, to improve extrapolation to a physical value, we choose to include the extra-fine ensemble in the RHQ analysis: X1. To use this additional ensemble, we perform the nonperturbative tuning procedure for the RHQ parameters m_0, c_P, and ζ as previously done for the other ensembles [25]. Measurements performed on the X1 ensemble make use of Grid [35, 36] and Hadrons [37].

This RHQ tuning process is not yet completed for this analysis, however at the current stage of this procedure, we find promising signals of the potential of X1 to aid in the analysis of the B_c decay constants, and potentially the light $B_{(s)}$ states as well. Examples of fits entering the tuning analysis are show in Figure 4.
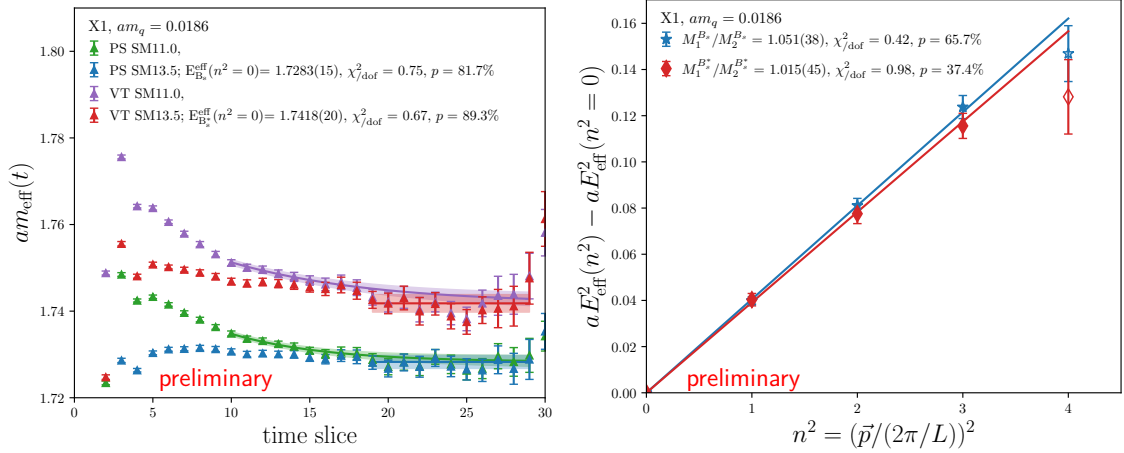

Figure 4: Examples of fits included in the tuning analysis on X1. *Left plot:* extraction of the ground state meson mass with $\vec{p}^2 = 0$ for pseudoscalar B_s and vector B_s^*. The valence quark is set to the unitary strange mass, $am_q = 0.0186$. Two correlators with different Gaussian-smearing radii are used in a combined fully-correlated fit and a first excited state is also included for the smaller smearing radius. *Right plot:* a fit to the slope of the continuum dispersion relation where ground state energies are first extracted for each integer square momentum n^2, and we fit to $n^2 \leq 3$. Tuned RHQ parameters enforce a slope equal to 1.

5. B_c Decay Constant

In analysing the B_c system, one finds a difference from B mesons with light/strange valence quarks in that the heavier c valence quark leads to higher statistical precision in the correlators, given the same number of measurements. However, we are instead more sensitive to systematic effects, in particular charm discretisation errors. In the left plot of Figure 5, one can see that the statistical precision is a factor ~ 2 higher than previously.

On each ensemble, we extract the decay amplitude at multiple charm quark masses and then on C we extrapolate to the physical charm mass, while on M, F, and X we bracket the physical value and interpolate. We define the physical charm point through the $\eta_c(1S)$ meson mass (neglecting disconnected diagrams), matching to the measured value $M_{\eta_c} = 2983.9(4)$ MeV [32]. Until the RHQ tuning is complete and we have finalised data on X1, we do not settle on a fit Ansatz for the combined continuum and physical charm extrapolation. In the right plot of Figure 5, we present the pseudoscalar decay amplitudes of the B_c meson on each ensemble. The different slopes one can see between ensembles indicate cut-off effects which need to be controlled in the final extrapolation. We use open symbols for the X1 data to indicate that these are not finalised until the RHQ tuning is finished, and therefore their vertical positioning will change in the final analysis. However the slope between the two data points indicates this ensemble will indeed be important in extrapolating to physical values.
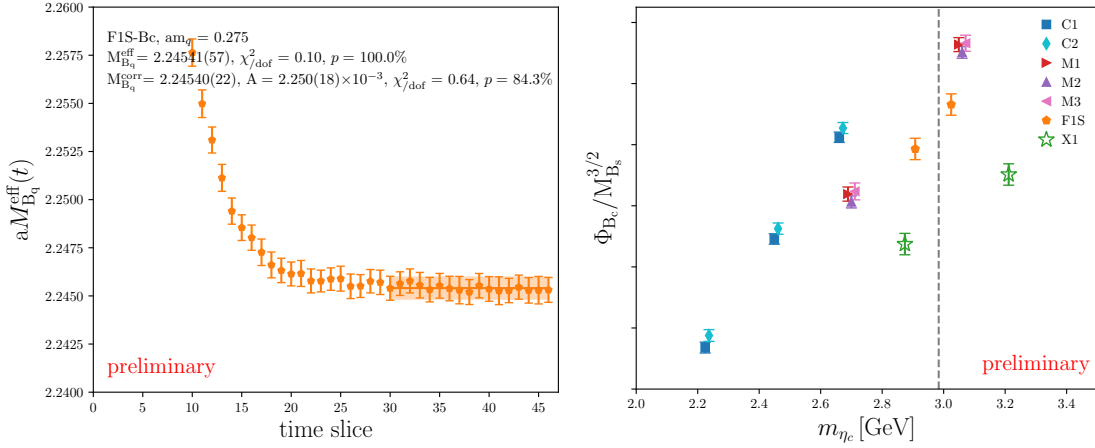
Figure 5: Analysis of the B_c pseudoscalar dimensionless decay amplitudes. *Left plot:* determination of the effective mass on F1S for a single charm mass. *Right plot:* collection of decay amplitudes on each ensemble for multiple charm quark masses, represented through the $\eta_c(1S)$ mass (excluding disconnected contributions). The open-symbol data are only representative while the X1 RHQ tuning is still in process.

6. Summary

B meson decay constants are important quantities for understanding the hadronic physics in weak decays of the SM. Here we have presented ongoing work to extract decay constants for both pseudoscalar and vector *B* mesons with light, strange, and charm valence quarks using the effective RHQ action to simulate physical *b* quarks. Analysis of pseudoscalar f_{B_q} for $q = l, s$ including isospin-breaking effects in the light quark is ongoing. Systematic effects for the B_c meson motivated the inclusion of the X1 ensemble where the nonperturbative tuning of the RHQ action parameters is in progress. In addition, we are working on extracting B^* vector meson states and determining their decay constants. Once we have collected all measurements, we will obtain renormalised continuum results for all decay constants, as well as interesting ratios such as the SU(3)-breaking estimate $f_{B_s}/f_{B^{0,+}}$ and the vector-to-pseudoscalar ratio $f_{B^*_{l,s,c}}/f_{B_{l,s,c}}$ where an important question remains as to which side of unity this quantity should lie.

Acknowledgments

References

[1] BABAR collaboration, B. Aubert et al., *Phys.Rev.* **D81** (2010) 051101 [0912.2453].

[2] BELLE collaboration, K. Hara et al., *Phys. Rev. D* **82** (2010) 071101 [1006.4201].

[3] BABAR collaboration, J. Lees et al., *Phys.Rev.* **D88** (2013) 031102 [1207.0698].

[4] BELLE collaboration, I. Adachi et al., *Phys.Rev.Lett.* **110** (2013) 131801 [1208.4678].

[5] BELLE collaboration, B. Kronenbitter et al., *Phys. Rev. D* **92** (2015) 051102 [1503.05613].

[6] BELLE collaboration, M. T. Prim et al., *Phys. Rev. D* **101** (2020) 032007 [1911.03186].

[7] W. Lucha et al., *J. Phys. G* **38** (2011) 105002 [1008.2698].

[8] P. Gelhausen et al., *Phys. Rev. D* **88** (2013) 014015 [1305.5432].

[9] B. Pullin et al., *JHEP* **09** (2021) 023 [2106.13617].

[10] Y. Aoki et al., 2111.09849.

[11] FERMILAB/MILC collaboration, A. Bazavov et al., *Phys. Rev.* **D98** (2018) 074512 [1712.09262].

[12] ETM collaboration, A. Bussone et al., *Phys. Rev.* **D93** (2016) 114505 [1603.04306].

[13] HPQCD collaboration, R. Dowdall et al., *Phys. Rev. Lett.* **110** (2013) 222003 [1302.2644].

[14] HPQCD collaboration, C. Hughes et al., *Phys. Rev.* **D97** (2018) 054509 [1711.09981].

[15] HPQCD collaboration, B. Colquhoun et al., *Phys. Rev.* **D91** (2015) 114509 [1503.05762].

[16] D. Becirevic et al., 1407.1019.

[17] RBC/UKQCD collaboration, T. Blum et al., *Phys. Rev.* **D93** (2016) 074505 [1411.7017].

[18] RBC/UKQCD collaboration, P. A. Boyle et al., *JHEP* **12** (2017) 008 [1701.02644].

[19] RBC/UKQCD collaboration, P. A. Boyle et al., 1812.08791.

[20] RBC/UKQCD collaboration, C. Allton et al., *Phys. Rev.* **D78** (2008) 114509 [0804.0473].

[21] RBC/UKQCD collaboration, Y. Aoki et al., *Phys.Rev.* **D83** (2011) 074508 [1011.0892].

[22] N. H. Christ et al., *Phys.Rev.* **D76** (2007) 074505 [hep-lat/0608006].

[23] H.-W. Lin et al., *Phys.Rev.* **D76** (2007) 074506 [hep-lat/0608005].

[24] A. X. El-Khadra et al., *Phys. Rev.* **D55** (1997) 3933 [hep-lat/9604004].

[25] RBC/UKQCD collaboration, Y. Aoki et al., *Phys. Rev.* **D86** (2012) 116003 [1206.2554].

[26] RBC/UKQCD collaboration, P. Boyle et al., *JHEP* **04** (2016) 037 [1602.04118].

[27] P. A. Boyle et al., *EPJ Web Conf.* **175** (2018) 13013 [1712.00862].

[28] S. Hashimoto et al., *Phys. Rev.* **D61** (1999) 014502 [hep-ph/9906376].

[29] A. X. El-Khadra et al., *Phys.Rev.* **D64** (2001) 014502 [hep-ph/0101023].

[30] RBC/UKQCD collaboration, N. H. Christ et al., *Phys.Rev.* **D91** (2015) 054502 [1404.4670].

[31] C. Lehner. Private communication, 2014.

[32] Particle Data Group collaboration, R. L. Workman et al., *PTEP* **2022** (2022) 083C01.

[33] RBC/UKQCD collaboration, J. M. Flynn et al., *Phys. Rev.* **D93** (2016) 014510 [1506.06413].

[34] Particle Data Group collaboration, P. A. Zyla et al., *PTEP* **2020** (2020) 083C01.

[35] P. Boyle et al., "github.com/paboyle/Grid: Grid."

[36] P. A. Boyle et al., *PoS* **LATTICE2015** (2016) 023.

[37] A. Portelli et al., *github.com/aportelli/hadrons: Hadrons v1.3*, Mar., 2022. 10.5281/zenodo.6382460.

[38] P. A. Boyle et al., *PoS* **LATTICE2015** (2016) 023.